Testing Platform for the Validation of Vertical Take-off and Vertical Landing (VTVL) Control Algorithms

A. Toader and G. Tecuceanu

***Abstract*—This paper presents preliminary results obtained during the development of a Vertical Take-Off and Vertical Landing (VTVL) demonstrator. The aim of this vehicle is to provide the experimenter with a testing platform for the validation of advanced control techniques related to reusable launchers and landers, and additionally for the assessment of visual navigation systems.**

***Index Terms*—Reusable launch vehicle, VTVL demonstrator, VTVL control algorithms.**

I. Introduction

A Reusable Launch Vehicle (RLV) is a type of LV capable of having partially or fully recoverable components, which are to be reintegrated in the system for later missions. Up to date, it has been demonstrated that roughly 70% of such a system can be recuperated.

The reusable launching technology its currently developed by the well know American company SapceX [1] which already demonstrated this concept by several real missions along with NASA.

The SpaceX first success was achieved in April 2014, when the controlled landing of the first stage of a launch vehicle on the ocean surface was made. The following year, in January-April, two more tests were carried out. This time the controlled landing of the first step of the rocket on a floating platform was not a success. On December 21, 2015, SpaceX recorded its first success when the first stage of the Falcon 9 rocket landed vertically on the Cape Canaveral launch platform.

To follow this new technology trend, INCAS (National Institute for Aerospace Research) has developed during a national project, a testing platform that allows the research of the new take off and landing control algorithms.

It worth to mention, once the flight control algorithm are successfully implemented, this test bed could be also used for the visual navigation systems assessment.

II. Design Principle

The design principle rely on the fly-fix-fly" approach, which allows INCAS team to gain insights for all the subsystems by making flight experiments.

Manuscript received May 20, 2018; revised June 20, 2018.

A. Toader and G. Tecuceanu are with the National Institute for Aerospace Research "Elie Carafoli", Bucharest, Romania (e-mail: toader.adrian@incas.ro, tecuceanu.george@incas.ro).

To this aim, we chose to develop a flying platform based on the turbojet engine, that is able to perform low speed, low altitude flights.

a) b)

Fig. 1. VTVL a) design, b) developed.

The vehicle overall dimensions are given in Fig. 1.

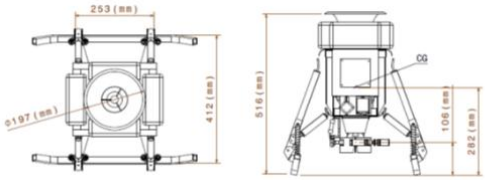

Fig. 2. Vehicle dimensions.

The lateral caps are the vital structural elements that close the structure of the vehicle. The caps were made in-house by the process of molding. Their composition consist of carbon fiber with epoxy resin with fabrics oriented to $0^o/90^o$. In the areas where mounting holes will be made, a metal insert is placed between the layers to distribute the force induced into the structure. On the sides of the caps, 6 captive nuts were mounted. These captive nuts are intended to provide mechanical resistance between the main structure and the landing gear.

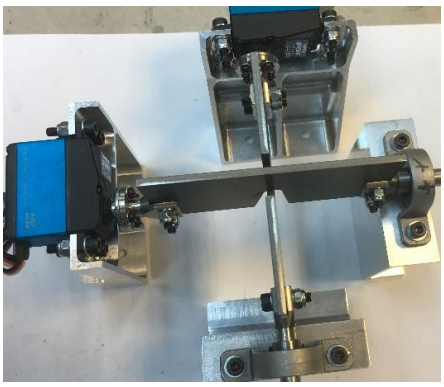

Fig. 3. Vehicle vanes.

A pair of vanes (Fig. 3) deflects the engine jet in order to create an aerodynamic torque which controls the vehicle attitude.

DOI: 10.7763/IJMO.2018.V8.657

III. Preliminary Vehicle Control Design

In this section we derive a simple position control law with emphasis on its implementation problem on the OBC (On Board Computer), problem which is inherently present on every numeric machine designed to embed the close loop control algorithm.

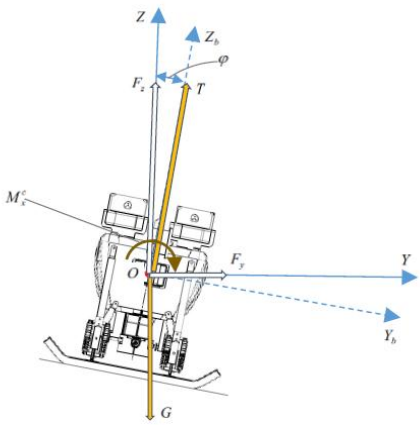

Fig. 4. Reference frames.

With respect to Fig. 4, the following equations [2] describe the vehicle motion in the longitudinal plane.

$$\begin{aligned} \ddot{y} &= \frac{1}{m} F_y \\ \ddot{\varphi} &= \frac{1}{I_{xx}} M_x^c \\ \ddot{z} &= \frac{1}{m}(F_z - G) \\ F_x &= T\cos\varphi \\ F_y &= T\sin\varphi \end{aligned} \tag{1}$$

Variables defined in the terrestrial frame zOy

F_x, F_y, G - forces acting on the vehicle (G is the weight of the vehicle);

$y, z[m]$ $\dot{y}, \dot{z}[m/s]$, $\ddot{y}, \ddot{z}\left[m/s^2\right]$ linear position, velocity and acceleration

Variables defined in the vehicle reference frame, $z_b O y_b$

$T[N]$ is the engine thrust, $M_x^c[Nm]$ is the control torque due to vanes deflection;

$\varphi[\deg]$ the angle between vehicle and terrestrial reference frames

$\omega_x \triangleq \dot{\varphi}[\deg/s]$ is the angular velocity

$\ddot{\varphi}\left[\deg/s^2\right]$ the angular acceleration

$m[Kg]$ vehicle mass,

$I_{xx}\left\lfloor Kgm^2 \right\rfloor$ is the vehicle moment of inertia w.r.t Ox_b axis

The nonlinear system of equations is linearized around an equilibrium point [3], which is chosen to be the stationary position of the vehicle at a given altitude. The equilibrium point is defined by the following state space variables $X_0 = [y \quad \dot{y} \quad z \quad \dot{z} \quad \varphi \quad \dot{\varphi}]^T = [0 \quad 0 \quad h_0 \quad 0 \quad 0 \quad 0]^T$ and control variables $U_0 = \left[T_0 \quad M_x^c\right]^T = [G \quad 0]^T$, respectively. The linearization procedure, yields the system

$$\begin{aligned} \dot{x}_1 &= x_2 \\ \dot{x}_2 &= \frac{1}{m} T_0 x_3 \\ \dot{x}_3 &= x_4 \\ \dot{x}_4 &= \frac{1}{I_{xx}} u_1 \\ \dot{x}_5 &= x_6 \\ \dot{x}_6 &= \frac{1}{m} u_2 \end{aligned} \tag{2}$$

where

$$x_1 \triangleq y,\ x_2 \triangleq \dot{y},\ x_3 \triangleq \varphi,\ x_4 \triangleq \dot{\varphi},\ x_5 \triangleq z,\ x_6 \triangleq \dot{z},\ u_1 \triangleq \delta T,\ u_2 \triangleq \delta M_x^c$$

Remark 1

In (2) the last two differential equations are decoupled from the other equations of the system.

Remark 2

To obtain a forward motion along Y axis, the vehicle should be first tilted around its X_b axis.

We are interested to control the lateral vehicle position only, while its altitude is constant. The linear system of equations (2) is written in the well known following form, in order to derive the controller gains K_{dp} and K_{da} , **Fig. 5.**

$$\begin{aligned} \dot{x} &= Ax + bu \\ y &= Cx \end{aligned} \tag{3}$$

where, $x = [x_1 \quad x_2 \quad x_3 \quad x_4]^T$ and

$$\mathbf{A} \triangleq \begin{bmatrix} 0 & 1 & 0 & 0 \\ 0 & 0 & T_0/m & 0 \\ 0 & 0 & 0 & 1 \\ 0 & 0 & 0 & 0 \end{bmatrix} \mathbf{b} \triangleq \begin{bmatrix} 0 \\ 0 \\ 0 \\ 1/I_{xx} \end{bmatrix}, \mathbf{C} = \mathbf{I}_{4\times 4}$$

The close loop vehicle positon control can be regarded as a two loop cascaded control system, the inner loop designed to preform vehicle attitude control (x_3^r is the attitude reference), while the outer loop tracks the position references, $y^r = x_1^r$.

The discretized of the continous system (3) with the sampling time T_s is

$$\begin{aligned} x(n+1) &= A_d x(n) + b_d u(n) \\ y(n) &= Cx(n) \end{aligned} \tag{4}$$

where $A_d = e^{AT_s}, b_d = \int_0^{T_s} e^{A\sigma} b d\sigma$

A linear quadratic controller [4] will be derived for the system (4)

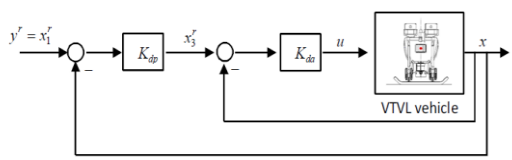

Fig. 5. Controller block diagram.

$$u(n) = -K_d x(n) = -\begin{bmatrix} K_{pd} & K_{ad} \end{bmatrix} \begin{bmatrix} x_1(n) \\ x_2(n) \\ x_3(n) \\ x_4(n) \end{bmatrix} \tag{5}$$

With the ideal control law (5), the close loop system is obtained

$$x(n+1) = (A_d - b_d K_d) x(n) \tag{6}$$

In reality the control is delayed one sample time (one step delay)

$$u(n) = -K_d x(n-1) \tag{7}$$

This delay can be included as an input delay for the system (4)

$$\begin{aligned} x(n+1) &= A_d x(n) + b_d u(n-1) \\ y(n) &= Cx(n) \end{aligned} \tag{8}$$

Introducing $u(n-1)$ as a suplimentary state i.e. $x_u(n) \triangleq u(n-1)$ the real open loop system is

$$x_e(n+1) = A_e x_e(n) + b_e u(n) \tag{9}$$

where $x_e(n) = \begin{bmatrix} x(n) & x_u(n) \end{bmatrix}^T$ and

$$A_e = \begin{bmatrix} A_d & b_d \\ \mathbf{0} & \mathbf{0} \end{bmatrix}, b_e = \begin{bmatrix} 0 \\ 1 \end{bmatrix}$$

The matrix of the closed loop system, derived form (9) and the control law (7) i.e. $u(n) = \begin{bmatrix} K_d & 0 \end{bmatrix} x_e(n)$, is

$$A_0 = \begin{bmatrix} A_d & b_d \\ -K_d & \mathbf{0} \end{bmatrix}$$

As it will be shown in the next section, for some weights on the performance index and sample time, the closed loop system performance degrades, or even worst, the matrix A_0 becomes unstable, due to computational time delay.

To compensate this time delay, inherently present in any discrete form of the controller, the control signal is updated using the predicted state of the system (8), thus

$$\begin{aligned} &u(n) = -K_d x(n+1) = \\ &-K_d A_d x(n) - K_d b_d u(n-1) = \\ &-K_d A_d x(n) - K_d b_d x_u(n) \end{aligned} \tag{10}$$

The closed loop form of the system (9) with the control law (10) is

$$x_e(n+1) = \bar{A}_0 x_e(n) \tag{11}$$

where

$$\bar{A}_0 = \begin{bmatrix} A_d & b_d \\ -K_d A_d & -K_d b_d \end{bmatrix}$$

Theorem 1, [5] If the ideal system (6) is asymptotically stable, then the system (11) is also asymptotically stable.

Moreover, the spectrum of $\bar{A}_0$ are the spectrum of A_0 plus a pole placed in the origin of complex plane.

IV. Numerical Results

The following numerical results prove the validity of the Theorem (1). In the mathematical models derived in the previous section, the aerodynamic effects (ram, drag) on the vehicle dynamics, as well as the vane actuator dynamics, are ignored.

Simulation input data:

$$m = 9.7550\,[\mathrm{Kg}],\ I_{xx} = 0.2277\,\lfloor \mathrm{Kgm}^2 \rfloor$$

Maximum control torque $M_x^c \max = 10\,[Nm]$

Minimum control torque $M_x^c \min = -10\,[Nm]$

Sample time $T_s = 0.08\,\mathrm{s}$

Weights on the performance index $Q = diag([1e4 \quad 1e2 \quad 5e6 \quad 7e4]); r = 400$

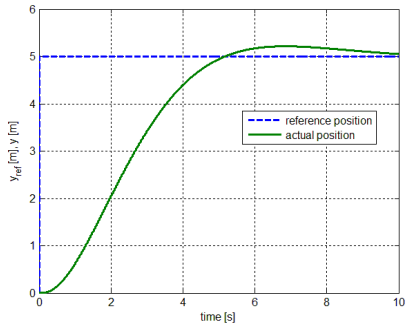

Fig. 6. Position tracking performance.

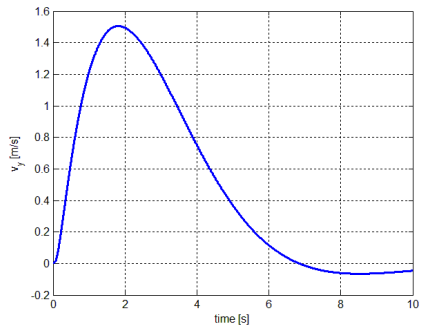

Fig. 7. Vehicle lateral velocity.

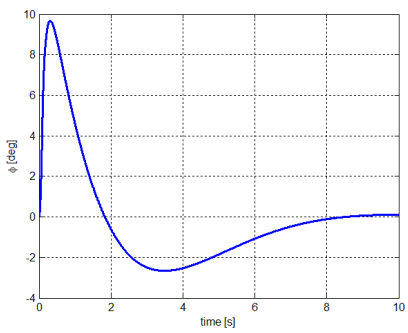

Fig. 8. Vehicle tilt angle.

Fig. 6 shows the position controller performance to track a 5 m step position reference. In Fig. 7 - Fig. 9, the vehicle

lateral velocity, angular position and angular rate are presented. These are the results of the same step reference position.

The control signal (Fig. 10) remains in the ±10Nm The close loop poles of the system (6) are:

$$\lambda_{disc} = \begin{bmatrix} -0.1691 & 0.505 & 0.96+0.036i & 0.96-0.036i \end{bmatrix}^T \quad (12)$$

These results were obtained for an ideal discrete control law (4) when there is no computational delay.

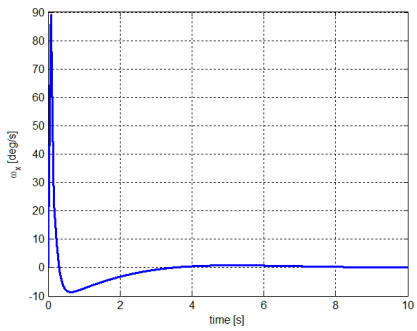

Fig. 9. Vehicle tilt rate.

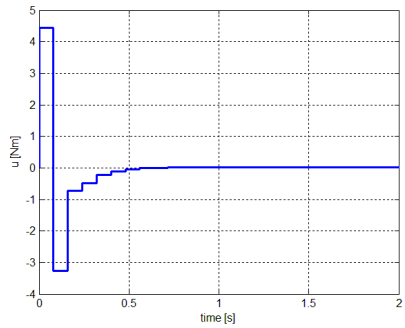

Fig. 10. Control torque.

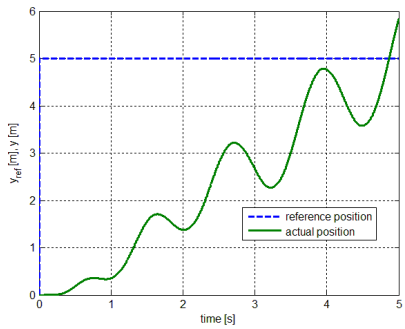

Fig. 11. Tracking performance – degraded

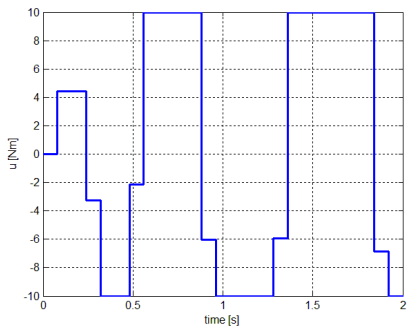

Fig. 12. Control torque – Saturated.

In the case when the computational time is implemented in the simulator (by an unit delay), the closed loop system becomes unstable (Fig. 11) and the control signal reaches its limits (Fig. 12).

The closed loop tracking performance is recovered (**Fig. 13**) when the system predicted state is fed into the controller (10).

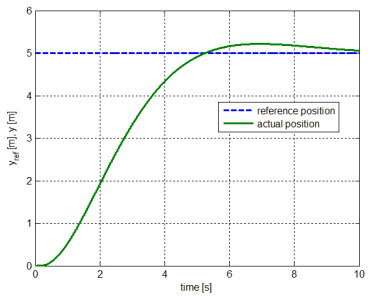

Fig. 13. Tracking performance – recovered.

The poles of the closed loop system (11) are:

$$\lambda_{disc} = \begin{bmatrix} 0 & -0.1691 & 0.505 & 0.96+0.036i & 0.96-0.036i \end{bmatrix} \quad (13)$$

V. Conclusion

The paper presents the INCAS activity related to the space programme. This activity concerns the development of a flying platform in order to prove the reusability concept in the case of a launcher system.

A key step on the path of cost reduction and the enhancement of the domain of applicability of the launcher is to embed new functional capabilities into software and control algorithms rather than to resort on expensive hardware components.

The first section of the paper tries to justify the research effort taking into account this new technological trend.

The vehicle is described in the section II, where its layout is underlined. Section III is focused on a "real problem" related to implementation of the control algorithm on the onboard computer. The numerical simulation outcomes, presented in the section IV, prove the theoretical results of the section III.

Acknowledgment

A. Toader would like to thank his younger colleagues Eng. Alexandru Persinaru and Eng. Alexandru Cismilianu for their commitment in the vehicle design and development.

References

[1] *** Falcon 9 Launch Vehicle PAYLOAD USER'S GUIDE, Rev. 2, SPACE X, 2015.

[2] B. Etkin, *Dynamics of Atmospheric Flight*, 2st ed., John Wiley & Sons, Inc., 1972.

[3] H. K. Khalil, *Nonlinear Systems*, 3th ed., Prentice-Hall, Upper Saddle River, New Jersey 07458, 2002.

[4] H. Kwakernaak and R. Sivan, *Linear Optimal Control Systems*, Wiley Interscience, New York, 1972.

[5] G. Tecuceanu, *Cercetari Privind Implementarea Algoritmilor de Control Automat Pe Modelul Functional*, Cod: C-599, INCAS internal report, ed. May 1997

Adrian Toader received a B.S. degree in 2005 and an M.S. degree in 2007 in avionics and aerospace Navigation from "Politehnica" University of Bucharest, Faculty of Aerospace Engineering. Currently, and PhD degree, in 2013 in Control Systems Engineering from University of Craiova, Faculty of Automation, Computers and Electronics. He worked from 2006 to present at National Institute for Aerospace Research "Elie Carafoli" Bucharest, Romania, Mechatronics department. His current interest are synthesis and implementation of the control laws for aerospace mechatronic systems, vibration control and health monitoring of the mechanical structures, aircraft flight control design and simulation, data acquisition, numerical simulation of physical systems models.

George Tecuceanu is the head of INCAS Mechatronics Department and he has over 40 years of scientific career. He graduated University Politehnica Bucharest - Faculty of Automatic Control and Computer Science.

His research interest is theoretical and applied control synthesis, mathematical modeling, numerical methods, optimization, modern methods of synthesis of automatic flight control systems and electro-hydraulic servomechanisms. User of Microsoft Word, Matlab with Simulink, Labview.

He obtained the Excellence Award from Aircraft Engineering and Aerospace Technology Journal, Great Britain, in 1999.